A search for high-mass resonances decaying to dimuons at CDF

T. Aaltonen,[24] J. Adelman,[14] T. Akimoto,[56] B. Álvarez González,[12] S. Amerio[w],[44] D. Amidei,[35] A. Anastassov,[39] A. Annovi,[20] J. Antos,[15] G. Apollinari,[18] A. Apresyan,[49] T. Arisawa,[58] A. Artikov,[16] W. Ashmanskas,[18] A. Attal,[4] A. Aurisano,[54] F. Azfar,[43] P. Azzurri[z],[47] W. Badgett,[18] A. Barbaro-Galtieri,[29] V.E. Barnes,[49] B.A. Barnett,[26] V. Bartsch,[31] G. Bauer,[33] P.-H. Beauchemin,[34] F. Bedeschi,[47] D. Beecher,[31] S. Behari,[26] G. Bellettini[x],[47] J. Bellinger,[60] D. Benjamin,[17] A. Beretvas,[18] J. Beringer,[29] A. Bhatti,[51] M. Binkley,[18] D. Bisello[w],[44] I. Bizjak[cc],[31] R.E. Blair,[2] C. Blocker,[7] B. Blumenfeld,[26] A. Bocci,[17] A. Bodek,[50] V. Boisvert,[50] G. Bolla,[49] D. Bortoletto,[49] J. Boudreau,[48] A. Boveia,[11] B. Brau[a],[11] A. Bridgeman,[25] L. Brigliadori,[44] C. Bromberg,[36] E. Brubaker,[14] J. Budagov,[16] H.S. Budd,[50] S. Budd,[25] S. Burke,[18] K. Burkett,[18] G. Busetto[w],[44] P. Bussey[k],[22] A. Buzatu,[34] K. L. Byrum,[2] S. Cabrera[u],[17] C. Calancha,[32] M. Campanelli,[36] M. Campbell,[35] F. Canelli,[18] A. Canepa,[46] B. Carls,[25] D. Carlsmith,[60] R. Carosi,[47] S. Carrillo[m],[19] S. Carron,[34] B. Casal,[12] M. Casarsa,[18] A. Castro[v],[6] P. Catastini[y],[47] D. Cauz[bb],[55] V. Cavaliere[y],[47] M. Cavalli-Sforza,[4] A. Cerri,[29] L. Cerrito[n],[31] S.H. Chang,[28] Y.C. Chen,[1] M. Chertok,[8] G. Chiarelli,[47] G. Chlachidze,[18] F. Chlebana,[18] K. Cho,[28] D. Chokheli,[16] J.P. Chou,[23] G. Choudalakis,[33] S.H. Chuang,[53] K. Chung,[13] W.H. Chung,[60] Y.S. Chung,[50] T. Chwalek,[27] C.I. Ciobanu,[45] M.A. Ciocci[y],[47] A. Clark,[21] D. Clark,[7] G. Compostella,[44] M.E. Convery,[18] J. Conway,[8] M. Cordelli,[20] G. Cortiana[w],[44] C.A. Cox,[8] D.J. Cox,[8] F. Crescioli[x],[47] C. Cuenca Almenar[u],[8] J. Cuevas[r],[12] R. Culbertson,[18] J.C. Cully,[35] D. Dagenhart,[18] M. Datta,[18] T. Davies,[22] P. de Barbaro,[50] S. De Cecco,[52] A. Deisher,[29] G. De Lorenzo,[4] M. Dell'Orso[x],[47] C. Deluca,[4] L. Demortier,[51] J. Deng,[17] M. Deninno,[6] P.F. Derwent,[18] G.P. di Giovanni,[45] C. Dionisi[aa],[52] B. Di Ruzza[bb],[55] J.R. Dittmann,[5] M. D'Onofrio,[4] S. Donati[x],[47] P. Dong,[9] J. Donini,[44] T. Dorigo,[44] S. Dube,[53] J. Efron,[40] A. Elagin,[54] R. Erbacher,[8] D. Errede,[25] S. Errede,[25] R. Eusebi,[18] H.C. Fang,[29] S. Farrington,[43] W.T. Fedorko,[14] R.G. Feild,[61] M. Feindt,[27] J.P. Fernandez,[32] C. Ferrazza[z],[47] R. Field,[19] G. Flanagan,[49] R. Forrest,[8] M.J. Frank,[5] M. Franklin,[23] J.C. Freeman,[18] I. Furic,[19] M. Gallinaro,[52] J. Galyardt,[13] F. Garberson,[11] J.E. Garcia,[21] A.F. Garfinkel,[49] K. Genser,[18] H. Gerberich,[25] D. Gerdes,[35] A. Gessler,[27] S. Giagu[aa],[52] V. Giakoumopoulou,[3] P. Giannetti,[47] K. Gibson,[48] J.L. Gimmell,[50] C.M. Ginsburg,[18] N. Giokaris,[3] M. Giordani[bb],[55] P. Giromini,[20] M. Giunta[x],[47] G. Giurgiu,[26] V. Glagolev,[16] D. Glenzinski,[18] M. Gold,[38] N. Goldschmidt,[19] A. Golossanov,[18] G. Gomez,[12] G. Gomez-Ceballos,[33] M. Goncharov,[54] O. González,[32] I. Gorelov,[38] A.T. Goshaw,[17] K. Goulianos,[51] A. Gresele[w],[44] S. Grinstein,[23] C. Grosso-Pilcher,[14] R.C. Group,[18] U. Grundler,[25] J. Guimaraes da Costa,[23] Z. Gunay-Unalan,[36] C. Haber,[29] K. Hahn,[33] S.R. Hahn,[18] E. Halkiadakis,[53] B.-Y. Han,[50] J.Y. Han,[50] F. Happacher,[20] K. Hara,[56] D. Hare,[53] M. Hare,[57] S. Harper,[43] R.F. Harr,[59] R.M. Harris,[18] M. Hartz,[48] K. Hatakeyama,[51] C. Hays,[43] M. Heck,[27] A. Heijboer,[46] J. Heinrich,[46] C. Henderson,[33] M. Herndon,[60] J. Heuser,[27] S. Hewamanage,[5] D. Hidas,[17] C.S. Hill[c],[11] D. Hirschbuehl,[27] A. Hocker,[18] S. Hou,[1] M. Houlden,[30] S.-C. Hsu,[29] B.T. Huffman,[43] R.E. Hughes,[40] U. Husemann,[36] M. Hussein,[36] U. Husemann,[61] J. Huston,[36] J. Incandela,[11] G. Introzzi,[47] M. Iori[aa],[52] A. Ivanov,[8] E. James,[18] B. Jayatilaka,[17] E.J. Jeon,[28] M.K. Jha,[6] S. Jindariani,[18] W. Johnson,[8] M. Jones,[49] K.K. Joo,[28] S.Y. Jun,[13] J.E. Jung,[28] T.R. Junk,[18] T. Kamon,[54] D. Kar,[19] P.E. Karchin,[59] Y. Kato,[42] R. Kephart,[18] J. Keung,[46] V. Khotilovich,[54] B. Kilminster,[18] D.H. Kim,[28] H.S. Kim,[28] H.W. Kim,[28] J.E. Kim,[28] M.J. Kim,[20] S.B. Kim,[28] S.H. Kim,[56] Y.K. Kim,[14] N. Kimura,[56] L. Kirsch,[7] S. Klimenko,[19] B. Knuteson,[33] B.R. Ko,[17] K. Kondo,[58] D.J. Kong,[28] J. Konigsberg,[19] A. Korytov,[19] A.V. Kotwal,[17] M. Kreps,[27] J. Kroll,[46] D. Krop,[14] N. Krumnack,[5] M. Kruse,[17] V. Krutelyov,[11] T. Kubo,[56] T. Kuhr,[27] N.P. Kulkarni,[59] M. Kurata,[56] S. Kwang,[14] A.T. Laasanen,[49] S. Lami,[47] S. Lammel,[18] M. Lancaster,[31] R.L. Lander,[8] K. Lannon[q],[40] A. Lath,[53] G. Latino[y],[47] I. Lazzizzera[w],[44] T. LeCompte,[2] E. Lee,[54] H.S. Lee,[14] S.W. Lee[t],[54] S. Leone,[47] J.D. Lewis,[18] C.-S. Lin,[29] J. Linacre,[43] M. Lindgren,[18] E. Lipeles,[46] A. Lister,[8] D.O. Litvintsev,[18] C. Liu,[48] T. Liu,[18] N.S. Lockyer,[46] A. Loginov,[61] M. Loreti[w],[44] L. Lovas,[15] D. Lucchesi[w],[44] C. Luci[aa],[52] J. Lueck,[27] P. Lujan,[29] P. Lukens,[18] G. Lungu,[51] L. Lyons,[43] J. Lys,[29] R. Lysak,[15] D. MacQueen,[34] R. Madrak,[18] K. Maeshima,[18] K. Makhoul,[33] T. Maki,[24] P. Maksimovic,[26] S. Malde,[43] S. Malik,[31] G. Manca[e],[30] A. Manousakis-Katsikakis,[3] F. Margaroli,[49] C. Marino,[27] C.P. Marino,[25] A. Martin,[61] V. Martin[l],[22] M. Martínez,[4] R. Martínez-Ballarín,[32] T. Maruyama,[56] P. Mastrandrea,[52] T. Masubuchi,[56] M. Mathis,[26] M.E. Mattson,[59] P. Mazzanti,[6] K.S. McFarland,[50] P. McIntyre,[54] R. McNulty[j],[30] A. Mehta,[30] P. Mehtala,[24] A. Menzione,[47] P. Merkel,[49] C. Mesropian,[51] T. Miao,[18] N. Miladinovic,[7] R. Miller,[36] C. Mills,[23] M. Milnik,[27] A. Mitra,[1] G. Mitselmakher,[19] H. Miyake,[56] N. Moggi,[6] C.S. Moon,[28] R. Moore,[18] M.J. Morello[x],[47] J. Morlok,[27] P. Movilla Fernandez,[18] J. Mülmenstädt,[29] A. Mukherjee,[18] Th. Muller,[27] R. Mumford,[26] P. Murat,[18] M. Mussini[v],[6] J. Nachtman,[18] Y. Nagai,[56] A. Nagano,[56] J. Naganoma,[56] K. Nakamura,[56] I. Nakano,[41] A. Napier,[57]

V. Necula,[17] J. Nett,[60] C. Neu[v],[46] M.S. Neubauer,[25] S. Neubauer,[27] J. Nielsen[g],[29] L. Nodulman,[2] M. Norman,[10]
O. Norniella,[25] E. Nurse,[31] L. Oakes,[43] S.H. Oh,[17] Y.D. Oh,[28] I. Oksuzian,[19] T. Okusawa,[42] R. Orava,[24]
S. Pagan Griso[w],[44] E. Palencia,[18] V. Papadimitriou,[18] A. Papaikonomou,[27] A.A. Paramonov,[14] B. Parks,[40]
S. Pashapour,[34] J. Patrick,[18] G. Pauletta[bb],[55] M. Paulini,[13] C. Paus,[33] T. Peiffer,[27] D.E. Pellett,[8] A. Penzo,[55]
T.J. Phillips,[17] G. Piacentino,[47] E. Pianori,[46] L. Pinera,[19] K. Pitts,[25] C. Plager,[9] L. Pondrom,[60] O. Poukhov*,[16]
N. Pounder,[43] F. Prakoshyn,[16] A. Pronko,[18] J. Proudfoot,[2] F. Ptohos[i],[18] E. Pueschel,[13] G. Punzi[x],[47] J. Pursley,[60]
J. Rademacker[c],[43] A. Rahaman,[48] V. Ramakrishnan,[60] N. Ranjan,[49] I. Redondo,[32] P. Renton,[43] M. Renz,[27]
M. Rescigno,[52] S. Richter,[27] F. Rimondi[v],[6] L. Ristori,[47] A. Robson,[22] T. Rodrigo,[12] T. Rodriguez,[46] E. Rogers,[25]
S. Rolli,[57] R. Roser,[18] M. Rossi,[55] R. Rossin,[11] P. Roy,[34] A. Ruiz,[12] J. Russ,[13] V. Rusu,[18] A. Safonov,[54]
W.K. Sakumoto,[50] O. Saltó,[4] L. Santi[bb],[55] S. Sarkar[aa],[52] L. Sartori,[47] K. Sato,[18] A. Savoy-Navarro,[45]
P. Schlabach,[18] A. Schmidt,[27] E.E. Schmidt,[18] M.A. Schmidt,[14] M.P. Schmidt*,[61] M. Schmitt,[39] T. Schwarz,[8]
L. Scodellaro,[12] A. Scribano[y],[47] F. Scuri,[47] A. Sedov,[49] S. Seidel,[38] Y. Seiya,[42] A. Semenov,[16] L. Sexton-Kennedy,[18]
F. Sforza,[47] A. Sfyrla,[25] S.Z. Shalhout,[59] T. Shears,[30] P.F. Shepard,[48] M. Shimojima[p],[56] S. Shiraishi,[14]
M. Shochet,[14] Y. Shon,[60] I. Shreyber,[37] A. Sidoti,[47] P. Sinervo,[34] A. Sisakyan,[16] A.J. Slaughter,[18] J. Slaunwhite,[40]
K. Sliwa,[57] J.R. Smith,[8] F.D. Snider,[18] R. Snihur,[34] A. Soha,[8] S. Somalwar,[53] V. Sorin,[36] J. Spalding,[18]
T. Spreitzer,[34] P. Squillacioti[y],[47] M. Stanitzki,[61] R. St. Denis,[22] B. Stelzer,[34] O. Stelzer-Chilton,[34] D. Stentz,[39]
J. Strologas,[38] G.L. Strycker,[35] D. Stuart,[11] J.S. Suh,[28] A. Sukhanov,[19] I. Suslov,[16] T. Suzuki,[56] A. Taffard[f],[25]
R. Takashima,[41] Y. Takeuchi,[56] R. Tanaka,[41] M. Tecchio,[35] P.K. Teng,[1] K. Terashi,[51] J. Thom[h],[18]
A.S. Thompson,[22] G.A. Thompson,[25] E. Thomson,[46] P. Tipton,[61] P. Ttito-Guzmán,[32] S. Tkaczyk,[18] D. Toback,[54]
S. Tokar,[15] K. Tollefson,[36] T. Tomura,[56] D. Tonelli,[18] S. Torre,[20] D. Torretta,[18] P. Totaro[bb],[55] S. Tourneur,[45]
M. Trovato,[47] S.-Y. Tsai,[1] Y. Tu,[46] N. Turini[y],[47] F. Ukegawa,[56] S. Vallecorsa,[21] N. van Remortel[b],[24] A. Varganov,[35]
E. Vataga[z],[47] F. Vázquez[m],[19] G. Velev,[18] C. Vellidis,[3] V. Veszpremi,[49] M. Vidal,[32] R. Vidal,[18] I. Vila,[12] R. Vilar,[12]
T. Vine,[31] M. Vogel,[38] I. Volobouev[t],[29] G. Volpi[x],[47] P. Wagner,[46] R.G. Wagner,[2] R.L. Wagner,[18] W. Wagner,[27]
J. Wagner-Kuhr,[27] T. Wakisaka,[42] R. Wallny,[9] S.M. Wang,[1] A. Warburton,[34] D. Waters,[31] M. Weinberger,[54]
J. Weinelt,[27] W.C. Wester III,[18] B. Whitehouse,[57] D. Whiteson[f],[46] A.B. Wicklund,[2] E. Wicklund,[18] S. Wilbur,[14]
G. Williams,[34] H.H. Williams,[46] P. Wilson,[18] B.L. Winer,[40] P. Wittich[h],[18] S. Wolbers,[18] C. Wolfe,[14]
T. Wright,[35] X. Wu,[21] F. Würthwein,[10] S.M. Wynne,[30] S. Xie,[33] A. Yagil,[10] K. Yamamoto,[42] J. Yamaoka,[53]
U.K. Yang[o],[14] Y.C. Yang,[28] W.M. Yao,[29] G.P. Yeh,[18] J. Yoh,[18] K. Yorita,[58] T. Yoshida,[42] G.B. Yu,[50]
I. Yu,[28] S.S. Yu,[18] J.C. Yun,[18] L. Zanello[aa],[52] A. Zanetti,[55] X. Zhang,[25] Y. Zheng[d],[9] and S. Zucchelli[v],[6]

(CDF Collaboration[†])

[1]*Institute of Physics, Academia Sinica, Taipei, Taiwan 11529, Republic of China*
[2]*Argonne National Laboratory, Argonne, Illinois 60439*
[3]*University of Athens, 157 71 Athens, Greece*
[4]*Institut de Fisica d'Altes Energies, Universitat Autonoma de Barcelona, E-08193, Bellaterra (Barcelona), Spain*
[5]*Baylor University, Waco, Texas 76798*
[6]*Istituto Nazionale di Fisica Nucleare Bologna,* [v]*University of Bologna, I-40127 Bologna, Italy*
[7]*Brandeis University, Waltham, Massachusetts 02254*
[8]*University of California, Davis, Davis, California 95616*
[9]*University of California, Los Angeles, Los Angeles, California 90024*
[10]*University of California, San Diego, La Jolla, California 92093*
[11]*University of California, Santa Barbara, Santa Barbara, California 93106*
[12]*Instituto de Fisica de Cantabria, CSIC-University of Cantabria, 39005 Santander, Spain*
[13]*Carnegie Mellon University, Pittsburgh, PA 15213*
[14]*Enrico Fermi Institute, University of Chicago, Chicago, Illinois 60637*
[15]*Comenius University, 842 48 Bratislava, Slovakia; Institute of Experimental Physics, 040 01 Kosice, Slovakia*
[16]*Joint Institute for Nuclear Research, RU-141980 Dubna, Russia*
[17]*Duke University, Durham, North Carolina 27708*
[18]*Fermi National Accelerator Laboratory, Batavia, Illinois 60510*
[19]*University of Florida, Gainesville, Florida 32611*
[20]*Laboratori Nazionali di Frascati, Istituto Nazionale di Fisica Nucleare, I-00044 Frascati, Italy*
[21]*University of Geneva, CH-1211 Geneva 4, Switzerland*
[22]*Glasgow University, Glasgow G12 8QQ, United Kingdom*
[23]*Harvard University, Cambridge, Massachusetts 02138*
[24]*Division of High Energy Physics, Department of Physics,*
University of Helsinki and Helsinki Institute of Physics, FIN-00014, Helsinki, Finland
[25]*University of Illinois, Urbana, Illinois 61801*

[26]The Johns Hopkins University, Baltimore, Maryland 21218
[27]Institut für Experimentelle Kernphysik, Universität Karlsruhe, 76128 Karlsruhe, Germany
[28]Center for High Energy Physics: Kyungpook National University, Daegu 702-701, Korea; Seoul National University, Seoul 151-742, Korea; Sungkyunkwan University, Suwon 440-746, Korea; Korea Institute of Science and Technology Information, Daejeon, 305-806, Korea; Chonnam National University, Gwangju, 500-757, Korea
[29]Ernest Orlando Lawrence Berkeley National Laboratory, Berkeley, California 94720
[30]University of Liverpool, Liverpool L69 7ZE, United Kingdom
[31]University College London, London WC1E 6BT, United Kingdom
[32]Centro de Investigaciones Energeticas Medioambientales y Tecnologicas, E-28040 Madrid, Spain
[33]Massachusetts Institute of Technology, Cambridge, Massachusetts 02139
[34]Institute of Particle Physics: McGill University, Montréal, Québec, Canada H3A 2T8; Simon Fraser University, Burnaby, British Columbia, Canada V5A 1S6; University of Toronto, Toronto, Ontario, Canada M5S 1A7; and TRIUMF, Vancouver, British Columbia, Canada V6T 2A3
[35]University of Michigan, Ann Arbor, Michigan 48109
[36]Michigan State University, East Lansing, Michigan 48824
[37]Institution for Theoretical and Experimental Physics, ITEP, Moscow 117259, Russia
[38]University of New Mexico, Albuquerque, New Mexico 87131
[39]Northwestern University, Evanston, Illinois 60208
[40]The Ohio State University, Columbus, Ohio 43210
[41]Okayama University, Okayama 700-8530, Japan
[42]Osaka City University, Osaka 588, Japan
[43]University of Oxford, Oxford OX1 3RH, United Kingdom
[44]Istituto Nazionale di Fisica Nucleare, Sezione di Padova-Trento, [w]University of Padova, I-35131 Padova, Italy
[45]LPNHE, Universite Pierre et Marie Curie/IN2P3-CNRS, UMR7585, Paris, F-75252 France
[46]University of Pennsylvania, Philadelphia, Pennsylvania 19104
[47]Istituto Nazionale di Fisica Nucleare Pisa, [x]University of Pisa, [y]University of Siena and [z]Scuola Normale Superiore, I-56127 Pisa, Italy
[48]University of Pittsburgh, Pittsburgh, Pennsylvania 15260
[49]Purdue University, West Lafayette, Indiana 47907
[50]University of Rochester, Rochester, New York 14627
[51]The Rockefeller University, New York, New York 10021
[52]Istituto Nazionale di Fisica Nucleare, Sezione di Roma 1, [aa]Sapienza Università di Roma, I-00185 Roma, Italy
[53]Rutgers University, Piscataway, New Jersey 08855
[54]Texas A&M University, College Station, Texas 77843
[55]Istituto Nazionale di Fisica Nucleare Trieste/Udine, [bb]University of Trieste/Udine, Italy
[56]University of Tsukuba, Tsukuba, Ibaraki 305, Japan
[57]Tufts University, Medford, Massachusetts 02155
[58]Waseda University, Tokyo 169, Japan
[59]Wayne State University, Detroit, Michigan 48201
[60]University of Wisconsin, Madison, Wisconsin 53706
[61]Yale University, New Haven, Connecticut 06520

We present a search for high-mass neutral resonances using dimuon data corresponding to an integrated luminosity of 2.3 fb^{-1} collected in $p\bar{p}$ collisions at $\sqrt{s} = 1.96$ TeV by the CDF II detector at the Fermilab Tevatron. No significant excess above the standard model expectation is observed in the dimuon invariant-mass spectrum. We set 95% confidence level upper limits on $\sigma \cdot BR(p\bar{p} \to X \to \mu\bar{\mu})$, where X is a boson with spin 0, 1, or 2. Using these cross section limits, we determine lower mass limits on sneutrinos in R-parity-violating supersymmetric models, Z' bosons, and Kaluza-Klein gravitons in the Randall-Sundrum model.

PACS numbers: 13.85.Rm, 13.85.Qk, 12.60.Cn, 14.70.Pw, 04.50.-h

[*]Deceased
[†]With visitors from [a]University of Massachusetts Amherst, Amherst, Massachusetts 01003, [b]Universiteit Antwerpen, B-2610 Antwerp, Belgium, [c]University of Bristol, Bristol BS8 1TL, United Kingdom, [d]Chinese Academy of Sciences, Beijing 100864, China, [e]Istituto Nazionale di Fisica Nucleare, Sezione di Cagliari, 09042 Monserrato (Cagliari), Italy, [f]University of California Irvine, Irvine, CA 92697, [g]University of California Santa Cruz,

Neutral resonances decaying to muons have historically been a source of major discoveries. They also occur in a variety of theoretical models which attempt to unify the standard model (SM) forces or explain the large gap between the SM and gravitational energy scales. The gauge group $SU(3)_C \times SU(2)_L \times U(1)_Y$ of the SM can be embedded in larger gauge groups such as $SU(5)$, $SO(10)$, and E_6, to achieve unification in a grand unified theory (GUT) [1–4]. In many schemes of GUT symmetry-breaking, $U(1)$ gauge groups survive to relatively low energies [2], leading to the prediction of neutral gauge vector bosons, generically referred to as Z' bosons. Such Z' bosons typically couple with electroweak strength to SM fermions, and can be observed at hadron colliders as narrow, spin-1, dimuon resonances from $q\bar{q} \to Z' \to \mu\bar{\mu}$. Many other models, such as the $SU(2)_L \times SU(2)_R \times U(1)_{B-L}$ gauge group of the left-right model [5], and the "little Higgs" models [6, 7], also predict heavy neutral gauge bosons.

Additional spatial dimensions are a possible explanation for the gap between the electroweak symmetry-breaking scale and the gravitational energy scale M_{Planck} [8, 9]. In the Randall-Sundrum (RS) scenario [9], the ground-state wave function of the graviton is localized on a three-dimensional "brane" separated in a fourth spatial dimension from the SM brane. The wave function varies exponentially in this fourth dimension, causing its overlap with the SM brane to be suppressed and explaining the apparent weakness of gravity and the large value of M_{Planck}. This model predicts excited Kaluza-Klein modes of the graviton which are localized on the SM brane. These modes appear as spin-2 resonances G^* in the process $q\bar{q} \to G^* \to \mu\bar{\mu}$, with a narrow intrinsic width when $k/M_{\text{Planck}} < 0.1$, where k^2 is the spacetime curvature in the extra dimension. In superstring theories with $\mathcal{O}(1)$ couplings, $k/M_{\text{Planck}} \approx 0.01$ [10].

Spin-0 resonances such as the sneutrino $\tilde{\nu}$ in the process $q\bar{q} \to \tilde{\nu} \to \mu\bar{\mu}$ are predicted by supersymmetric theories with R-parity violation [11], where R-parity is a multiplicative quantum number that is conserved in interactions with an even number of supersymmetric particles. Scalar Higgs bosons in the SM and its extensions can be produced as resonances and decay to dimuons.

The most sensitive direct searches for high-mass boson resonances, which have previously been performed at the Tevatron, have set 95% confidence level (C.L.) lower limits on the masses $M_{Z'}$, M_{G^*}, and $M_{\tilde{\nu}}$ of Z' bosons, RS gravitons, and sneutrinos, respectively. The previous dimuon publication from CDF II, based on ≈ 200 pb^{-1} of integrated luminosity [12], setting limits that vary from 170 GeV to 885 GeV depending on the boson spin and couplings to the SM fermions. Other dilepton and diphoton decay channels have also been explored at the Tevatron [13, 14]. Using an order of magnitude more data, we present in this Letter the most sensitive direct search to date for Z', G^*, and $\tilde{\nu}$ bosons at high mass.

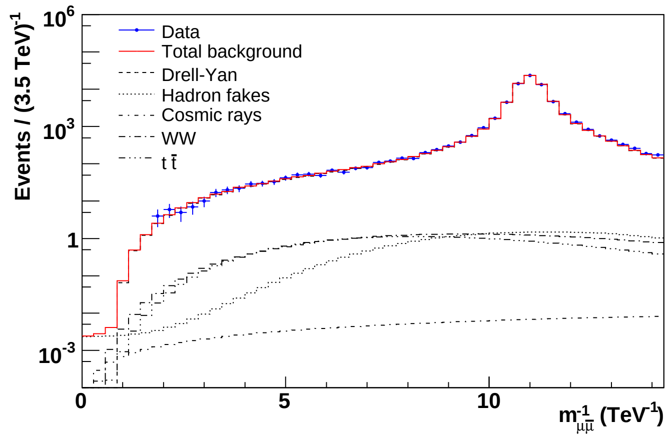

FIG. 1: The distribution of $m_{\mu\bar{\mu}}^{-1}$ (TeV^{-1}) for the observed data (points), the individual backgrounds (dotted or dashed histograms) and the summed background (solid histogram). The Z boson peak is prominently seen. The inverse mass distribution has the useful feature that the detector resolution is approximately constant (≈ 0.17 TeV^{-1}) over the range shown in the plot.

This analysis uses data corresponding to an integrated luminosity of 2.3 fb^{-1}, collected in $p\bar{p}$ collisions at $\sqrt{s} = 1.96$ TeV by the CDF II detector [15, 16] at the Tevatron. CDF II is a magnetic spectrometer surrounded by calorimeters and muon detectors. We use the central drift chamber (COT) [17], the central calorimeter [18], and the muon detectors [19] for identification and measurement of muons with $|\eta| < 1$ [20]. The online muon event selection (trigger) requires a COT track with $p_T > 18$ GeV [20], and matching muon detector hits. We select a pair of oppositely-charged muons, each with a COT track with $p_T > 30$ GeV passing quality requirements, and a minimum-ionization signal in the calorimeter. Cosmic rays are rejected using COT hit timing [21]. The dimuon signal sample consists of 68150 events in the dimuon invariant mass control region $70 < m_{\mu\bar{\mu}} < 100$ GeV, where

Santa Cruz, CA 95064, [h]Cornell University, Ithaca, NY 14853, [i]University of Cyprus, Nicosia CY-1678, Cyprus, [j]University College Dublin, Dublin 4, Ireland, [k]Royal Society of Edinburgh/Scottish Executive Support Research Fellow, [l]University of Edinburgh, Edinburgh EH9 3JZ, United Kingdom, [m]Universidad Iberoamericana, Mexico D.F., Mexico, [n]Queen Mary, University of London, London, E1 4NS, England, [o]University of Manchester, Manchester M13 9PL, England, [p]Nagasaki Institute of Applied Science, Nagasaki, Japan, [q]University of Notre Dame, Notre Dame, IN 46556, [r]University de Oviedo, E-33007 Oviedo, Spain, [s]Texas Tech University, Lubbock, TX 79409, [t]IFIC(CSIC-Universitat de Valencia), 46071 Valencia, Spain, [u]University of Virginia, Charlottesville, VA 22904, [cc]On leave from J. Stefan Institute, Ljubljana, Slovenia,

the $p\bar{p} \to Z \to \mu\bar{\mu}$ process dominates, and 3804 events in the search region $m_{\mu\bar{\mu}} > 100$ GeV.

The alignment of the COT is performed using a pure sample of high-momentum cosmic-ray muons, in order to obtain the best possible dimuon mass resolution. Each muon's complete trajectory is fitted to a single helix [21]. The fits are used to determine the relative locations of the sense wires, including gravitational and electrostatic displacements, with a statistical accuracy of a few microns. We constrain remaining misalignments, which cause a bias in the track curvature, by comparing $\langle E/p \rangle$ [20] for electrons and positrons. The tracker momentum scale and resolution is measured by template-fitting the $Z \to \mu\bar{\mu}$ mass peak, and calibrating to the world average values [22] of the Z boson mass and width.

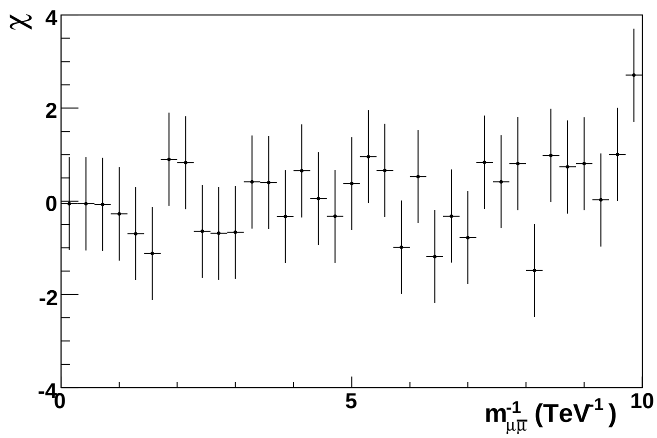

FIG. 2: The difference between the distributions of $m_{\mu\bar{\mu}}^{-1}$ (TeV^{-1}) for the observed data and the summed background, divided by the expected statistical uncertainty in each bin. All vertical error bars have unit size. The p-value (defined in the text) of the largest deviation (which occurs at $m_{\mu\bar{\mu}} \sim 103$ GeV as seen above) is 6.6%.

For a resonance with electroweak coupling and mass above 200 GeV, the observed width of the $m_{\mu\bar{\mu}}$ distribution is dominated by the track curvature resolution, resulting in an approximately constant resolution of $\delta m_{\mu\bar{\mu}}^{-1} \approx 0.17$ TeV^{-1}. Our search strategy is to construct templates of the observable $m_{\mu\bar{\mu}}^{-1}$ distribution for a range of boson Breit-Wigner pole masses, add the background distributions to the templates, and compare the templates to the $m_{\mu\bar{\mu}}^{-1}$ distribution from the data in the search region $m_{\mu\bar{\mu}} > 100$ GeV. The simulated templates (including backgrounds) are normalized to the data in the 70 GeV $< m_{\mu\bar{\mu}} <$ 100 GeV region, thus cancelling several sources of systematic uncertainty.

We determine the most likely number of signal events (N_S), and the corresponding confidence intervals [23], from the binned Poisson likelihood [16] for the observed data to be produced by a sum of signal and background templates. The use of the constant-resolution variable $m_{\mu\bar{\mu}}^{-1}$ simplifies the optimization of the template binning and the scan over the boson pole masses.

Signal and SM Drell-Yan background distributions are evaluated using a specialized Monte Carlo (MC) simulation [16] of boson production and decay, and of the detector response to the leptons and hadrons. The kinematics of boson production and decay are obtained from the PYTHIA [24] event generator using the CTEQ6M [25] set of parton distribution functions. QED radiation is simulated [16] based on the WGRAD program [26]. The MC performs a detailed hit-level simulation of the lepton tracks. COT hits are generated according to their resolution (≈ 150 μm) and measured efficiencies, and a helix fit is performed (as it is in data) to simulate the reconstructed track. We apply a mass-dependent next-to-next-to-leading order (NNLO) multiplicative correction (K-factor) [27] to the SM Drell-Yan background.

Z' model	Z' mass limit	RS graviton k/M_{Planck}	graviton mass limit	$\tilde{\nu}$ $\lambda^2 \cdot BR$	$\tilde{\nu}$ mass limit
Z'_I	789	0.01	293	0.0001	278
Z'_{sec}	821	0.015	409	0.0002	397
Z'_N	861	0.025	493	0.0005	457
Z'_ψ	878	0.035	651	0.001	541
Z'_χ	892	0.05	746	0.002	662
Z'_η	982	0.07	824	0.005	751
Z'_{SM}	1030	0.1	921	0.01	810

TABLE I: 95% C.L. lower limits on Z', graviton, and sneutrino masses (in GeV) for various model parameters [9, 11, 33]. For the R-parity-violating sneutrino model, λ is the $d\bar{d}\tilde{\nu}$ coupling and BR denotes the $\tilde{\nu} \to \mu\bar{\mu}$ branching ratio.

The SM production processes for W^+W^- [28] and $t\bar{t}$ [29] have small contributions, and are evaluated using their NLO cross sections, PYTHIA, and a detector simulation based on GEANT [30]. Misidentification backgrounds result from cosmic rays, QCD jets, and π/K decays-in-flight (DIF). We evaluate the shape of the cosmic-ray background from a large sample of cosmic rays identified with the COT-timing-based algorithm [21], and normalize it to the data using events with large Δt_0, where Δt_0 is the difference between the muons' reconstructed time at the beam axis under the assumption that both muons propagate outwards. In cosmic ray events, one of the muons is propagating inwards, resulting in a large reconstructed Δt_0. The $m_{\mu\bar{\mu}}^{-1}$ shape of misidentified jets is evaluated from a large sample of inclusive jet events. Decays-in-flight within the COT active volume generate a kink along the helical trajectory, resulting in a mismeasurement of the track curvature. For large reconstructed momenta, the measured DIF curvature distribution is approximately uniform and leads to a flat $m_{\mu\bar{\mu}}^{-1}$ spectrum. The kinks in DIF tracks allow most of them to be rejected using their abnormal COT-hit pattern and large χ^2 of the track fit. The jet and DIF backgrounds are normalized using the number of same-charge dimuon events observed at low and high mass respectively.

Figure 1 shows the $m_{\mu\bar{\mu}}^{-1}$ distributions of the observed data and the expected backgrounds, which are in good agreement (as shown in Fig. 2). A resonance whose observed width is dominated by detector resolution would appear as a peak spanning approximately three bins. The likelihood-based fitter finds no significant excess. We use background-only ensembles of simulated events, each with the statistics of the data sample, to evaluate the probability of statistical fluctuations anywhere in the search region generating a discrepancy at least as significant as the largest discrepancy found in the data. We find this probability ("p-value") to be 6.6% and we conclude that the observed data are statistically consistent with the SM expectation. A companion Letter [31] shows the dielectron m_{ee} spectrum from CDF II data corresponding to 2.5 fb^{-1} of integrated luminosity, where the largest discrepancy with the expected background occurs at $m_{ee} \sim 240$ GeV. Figure 2 shows that the dimuon data are consistent with the expectation near this mass to better than 1σ in statistical precision. The sensitivity of the dielectron analysis for a spin-1 resonance at this mass is $\approx 20\%$ better than the dimuon analysis reported here.

The likelihood fitter determines the 95% C.L. upper limit on the number of signal events, for each value of the resonance pole mass. We convert these limits to limits on $\sigma \cdot BR(\tilde{\nu} \to \mu\bar{\mu})$, $\sigma \cdot BR(Z' \to \mu\bar{\mu})$, and $\sigma \cdot BR(G^* \to \mu\bar{\mu})$ using the total acceptance as a function of pole mass, and dividing by the observed number of $Z \to \mu\bar{\mu}$ events. The acceptance is verified with the detailed GEANT-based simulation of the detector, as well as comparisons to data distributions. The muon identification efficiency is cross-checked using a pure data sample of Z bosons triggered by one identified muon. The simulation reproduces the muon efficiency as a function of muon p_T. The total acceptance, including kinematic and fiducial acceptance and dimuon identification efficiency, increases from $\approx 13\%$ at the Z boson pole to $\approx 40\%$ for a Z' pole mass of 1 TeV, and decreases for higher pole masses due to the kinematic limit of the parton collisions. The lepton η [20] distribution obtained from spin-2 graviton decay is more central than the distribution obtained from spin-1 boson decay. The total acceptance for the graviton increases from $\approx 20\%$ for a pole mass of 90 GeV to $\approx 45\%$ for a pole mass of 1 TeV. The 95% C.L. upper limits on $\sigma \cdot BR(\tilde{\nu} \to \mu\bar{\mu})$, $\sigma \cdot BR(Z' \to \mu\bar{\mu})$, and $\sigma \cdot BR(G^* \to \mu\bar{\mu})$ are shown in Fig. 3 as functions of M^{-1}, where M is the pole mass. The dominant mass-dependent systematic uncertainties arise from parton distribution functions (16%), the NNLO K-factor (9%) [27], QED radiative corrections (3%) [32], and acceptance (3%), all quoted at 1 TeV. These uncertainties are incorporated as functions of $m_{\mu\bar{\mu}}$ and increase monotonically beyond the normalization region at 100 GeV. Uncertainties on the momentum scale and resolution, and on the non-Drell-Yan background predictions, have a negligible effect on the search.

Our signal templates have been generated with a resonance pole width $\Gamma = 2.8\% \times M$, based on the SM Z boson width. Thus our signal scan probes an observed width of $\approx [17\%(M/\text{TeV}) \oplus 2.8\%]\ M$. In a model where the observed width increases by a factor x, the cross section limits would increase by about a factor of $\sqrt{x}$.

We use PYTHIA to compute the theoretical cross sections for production of Z' bosons predicted by E_6 models [33] or having the same couplings to SM fermions as the Z boson, as well as G^* production cross sections for various k/M_{Planck} values. We apply the NNLO K-factor to these LO cross sections. The NLO $\tilde{\nu}$ production cross sections are obtained from [11]. From the intersection of the observed limits and the theoretical cross section curves, we derive the boson mass limits shown in Table I.

In conclusion, we have presented a direct search for high-mass neutral resonances with spin-0, 1, and 2, using an integrated luminosity of 2.3 fb^{-1} collected by the CDF II detector. Our dimuon invariant mass spectrum is consistent with the SM expectation. We set the world's tightest constraints on Z' bosons in various models, on Kaluza-Klein graviton modes in the RS model, and on sneutrinos in R-parity violating supersymmetric models. At 95% C.L., we exclude $100 < M_{Z'} < 982$ GeV for a Z'_η boson of the E_6 model, $100 < M_{G^*} < 921$ GeV for $k/M_{\text{Planck}} = 0.1$, and $100 < M_{\tilde{\nu}} < 810$ GeV for $\lambda^2 \cdot BR(\tilde{\nu} \to \mu\bar{\mu}) = 0.01$, where λ is the $d\bar{d}\tilde{\nu}$ coupling and BR denotes the $\tilde{\nu} \to \mu\bar{\mu}$ branching ratio.

We thank the Fermilab staff and the technical staffs of the participating institutions for their vital contributions. This work was supported by the U.S. Department of Energy and National Science Foundation; the Italian Istituto Nazionale di Fisica Nucleare; the Ministry of Education, Culture, Sports, Science and Technology of Japan; the Natural Sciences and Engineering Research Council of Canada; the National Science Council of the Republic of China; the Swiss National Science Foundation; the A.P. Sloan Foundation; the Bundesministerium für Bildung und Forschung, Germany; the Korean Science and Engineering Foundation and the Korean Research Foundation; the Science and Technology Facilities Council and the Royal Society, UK; the Institut National de Physique Nucleaire et Physique des Particules/CNRS; the Russian Foundation for Basic Research; the Ministerio de Ciencia e Innovación, Spain; the Slovak R&D Agency; and the Academy of Finland.

[1] J. L. Rosner, Phys. Rev. D **35**, 2244 (1987).
[2] F. del Aguila, M. Quiros, and F. Zwirner, Nucl. Phys. **B287**, 419 (1987); J. L. Hewett, and T. G. Rizzo, Phys.

Rep. **183**, 193 (1989).
[3] J. Erler *et al.*, Phys. Rev. D **66**, 015002 (2002); T. Han *et al.*, Phys. Rev. D **70**, 115006 (2004).
[4] J. Kang and P. Langacker, Phys. Rev. D **71**, 035014 (2005).
[5] R. N. Mohapatra and J. C. Pati, Phys. Rev. D **11**, 566 (1975); G. Senjanovic and R. N. Mohapatra, Phys. Rev. D **12**, 1502 (1975); R. N. Mohapatra and G. Senjanovic, Phys. Rev. D **23**, 165 (1981).
[6] N. Arkani-Hamed *et al.*, J. High Energy Phys. 07, 034 (2002).
[7] T. Han *et al.*, Phys. Rev. D **67**, 095004 (2003).
[8] N. Arkani-Hamed, S. Dimopoulos, and G. Dvali, Phys. Lett. B **429**, 263 (1998).
[9] L. Randall and R. Sundrum, Phys. Rev. Lett. **83**, 4690 (1999); L. Randall and R. Sundrum, Phys. Rev. Lett. **83**, 3370 (1999).
[10] H. Davoudiasl, J. L. Hewett and T. G. Rizzo, Phys. Rev. Lett. **84**, 2080 (2000).
[11] D. Choudhury, S. Majhi, and V. Ravindran, Nucl. Phys. B **660**, 343 (2003).
[12] A. Abulencia *et al.* (CDF Collaboration), Phys. Rev. Lett. **95**, 252001 (2005).
[13] T. Aaltonen *et al.* (CDF Collaboration), Phys. Rev. Lett. **99**, 171802 (2007); T. Aaltonen *et al.* (CDF Collaboration), Phys. Rev. Lett. **99**, 171801 (2007); A. Abulencia *et al.* (CDF Collaboration), Phys. Rev. Lett. **96**, 211801 (2006); D. Acosta *et al.* (CDF Collaboration), Phys. Rev. Lett. **95**, 131801 (2005).
[14] V. M. Abazov *et al.* (D0 Collaboration), Phys. Rev. Lett. **100**, 091802 (2008).
[15] A. Abulencia *et al.* (CDF Collaboration), J. Phys. G **34**, 2457 (2007).
[16] T. Aaltonen *et al.* (CDF Collaboration), Phys. Rev. D **77**, 112001 (2008).
[17] T. Affolder *et al.*, Nucl. Instrum. Methods A **526**, 249 (2004).
[18] F. Abe *et al.* (CDF Collaboration), Nucl. Instrum. Methods A **271**, 387 (1988).
[19] G. Ascoli *et al.*, Nucl. Instrum. Methods A **268**, 33 (1988).
[20] Pseudorapidity is defined as $\eta = -\ln[\tan(\theta/2)]$, where θ is the polar angle from the beam axis. Track momentum p transverse to the beam is denoted p_T. We use the convention $\hbar = c = 1$.
[21] A. V. Kotwal, H. K. Gerberich, and C. Hays, Nucl. Instrum. Methods A **506**, 110 (2003).
[22] S. Schael *et al.* (ALEPH, DELPHI, L3, OPAL and SLD Collaborations), Phys. Rep. **427**, 257 (2006) and references therein.
[23] G. J. Feldman and R. D. Cousins, Phys. Rev. D **57**, 3873 (1998).
[24] T. Sjöstrand, Comput. Phys. Commun. **82**, 74 (1994), version 6.208.
[25] J. Pumplin *et al.*, J. High Energy Phys. **0207**, 012 (2002).
[26] U. Baur, S. Keller, and D. Wackeroth, Phys. Rev. D **59**, 013002 (1998).
[27] M. Carena, A. Daleo, B. A. Dobrescu, and T. M. P. Tait, Phys. Rev. D **70**, 093009 (2004).
[28] J. M. Campbell and R. K. Ellis, Phys. Rev. D **60**, 113006 (1999), MCFM version 3.4.5.
[29] R. Bonciani, S. Catani, M. L. Mangano, and P. Nason, Nucl. Phys. B **529**, 424 (1998); M. Cacciari *et al.*, J. High Energy Phys. 04, 068 (2004).
[30] R. Brun and F. Carminati, CERN Program Library Long Writeup, W5013, 1993 (unpublished), version 3.15.
[31] T. Aaltonen *et al.* (CDF Collaboration), arXiv:0810.2059, submitted for publication in Phys. Rev. Lett.
[32] U. Baur, O. Brein, W. Hollik, C. Schappacher, and D. Wackeroth, Phys. Rev. D **65**, 033007 (2002), Fig. 3(b).
[33] The couplings we use are detailed in C. Ciobanu *et al.*, FERMILAB-FN-0773-E (2005).

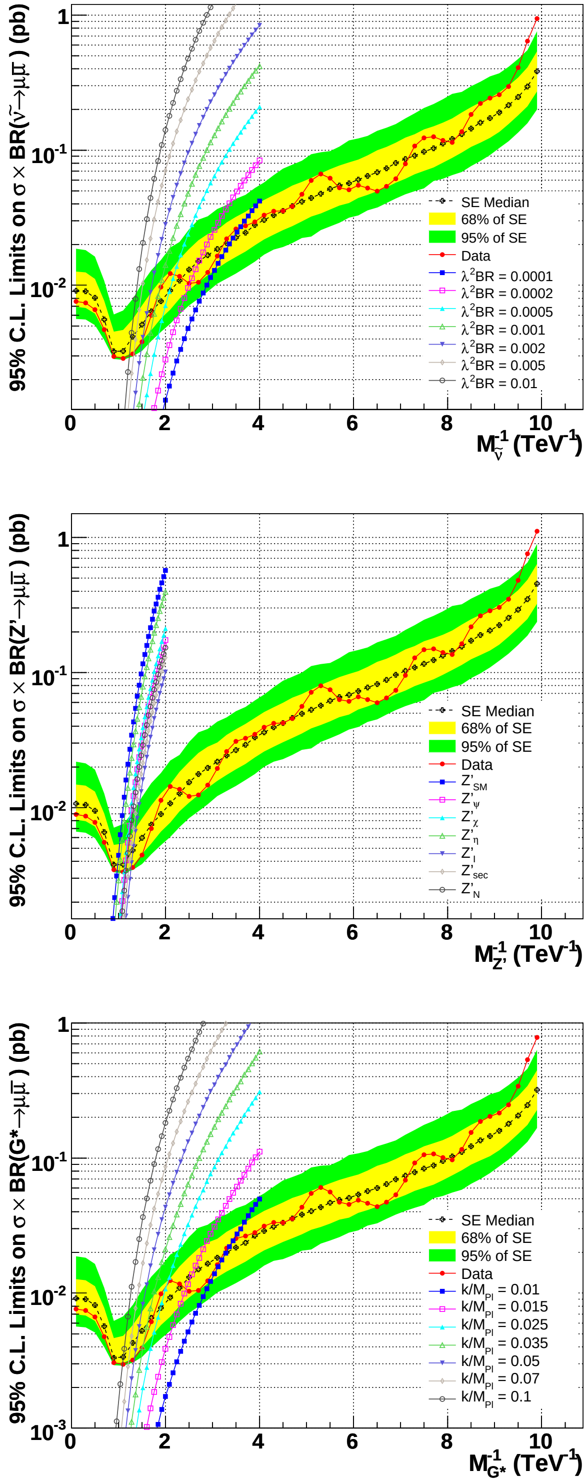

FIG. 3: The 95% C.L. upper limits on $\sigma \cdot BR(\tilde{\nu} \rightarrow \mu\bar{\mu})$ vs $M_{\tilde{\nu}}^{-1}$ (top), $\sigma \cdot BR(Z' \rightarrow \mu\bar{\mu})$ versus $M_{Z'}^{-1}$ (middle), and $\sigma \cdot BR(G^{*} \rightarrow \mu\bar{\mu})$ versus $M_{G^{*}}^{-1}$ (bottom). Also shown are the theoretical cross sections for various model parameter values [9, 11, 33]. The expected limits and ranges of limits, as derived from simulated experiments (SE), are shown for comparison.